J. Phys. B: At. Mol. Opt. Phys. **23** (1990) 2305–2320. Printed in the UK

Optical potentials in ion–atom collisions: II. Effective one-electron systems†

H Ast, H J Lüdde and R M Dreizler
Institut für Theoretische Physik der Universität, Frankfurt, West Germany

Received 20 July 1989, in final form 12 April 1990

Abstract. The optical model allows an extension of truncated coupled-channel calculations to energies for which ionisation channels become important. Collisions between ground-state and metastable (2s) hydrogen atoms and rare gases (helium, neon, argon) are investigated on the basis of a one-centre optical potential. We present results for direct excitation of hydrogen as well as for electron loss from hydrogen.

1. Introduction

The different reaction channels occurring in the collision of atomic hydrogen with rare-gas atoms can be divided into three classes.

(i) Singly inelastic processes with the rare gas remaining in its ground state:

$$\begin{aligned} &\mathrm{H + A \rightarrow H^* + A} \\ &\mathrm{H + A \rightarrow H^+ + A + e^-}. \end{aligned} \tag{1}$$

(ii) Singly inelastic processes with the hydrogen in its initial state:

$$\begin{aligned} &\mathrm{H + A \rightarrow H + A^*} \\ &\mathrm{H + A \rightarrow H + A^{\mathit{q}+} + \mathit{q}e^-}. \end{aligned} \tag{2}$$

(iii) Doubly inelastic processes, in which both collision partners are excited or ionised:

$$\begin{aligned} &\mathrm{H + A \rightarrow H^* + A^*} \\ &\mathrm{H + A \rightarrow H^+ + A^* + e^-} \\ &\mathrm{H + A \rightarrow H^* + A^{\mathit{q}+} + \mathit{q}e^-} \\ &\mathrm{H + A \rightarrow H^+ + A^{\mathit{q}+} + (\mathit{q}+1)e^-}. \end{aligned} \tag{3}$$

In most experimental data available (Allison 1958, Barnett and Reynolds 1958, Berkner *et al* 1964, Smythe and Toevs 1965, Stier and Barnett 1965, Toburen *et al* 1968, Dose *et al* 1968, Orbeli *et al* 1970, Gilbody *et al* 1971, Birely and McNeal 1972, Hughes and Choe 1972 a,b, Hughes etal 1972, Gilbody and Corr 1974, Acerbi *et*

† Work supported in part by the Deutsche Forschungsgemeinschaft.

al 1974, McKee *et al* 1979, Duncan and Menendez 1979, Hill *et al* 1979 a,b, 1980) only the projectile state is analysed after the collision process. The corresponding inclusive total cross sections for excitation and ionisation of the hydrogen atom thus contain contributions from all the reactions indicated under (i) and (iii).

For the system H+He one obtains agreement with experimental data for both direct excitation of the hydrogen atom and electron loss from hydrogen in the first Born approximation (Levy 1969a, Bell *et al* 1969, 1973, 1974) for energy values above 10 keV, if all singly and doubly inelastic processes are taken into account. Results for direct excitation obtained in close coupling calculations with a small basis set (four AO basis states) underestimate the experimental data for impact energies above 20 keV, as they only account for selected singly inelastic channels. If one adds the contribution of the corresponding doubly inelastic processes, obtained in the first Born approximation, one again finds (Levy 1969a) good agreement with the inclusive experimental data.

The situation is different for the collision systems H+Ne and H+Ar. Electron-loss cross sections are overestimated by the first Born approximation for all but the highest impact energies. Direct excitation cross sections are overestimated by the first Born and the small-scale close coupling calculation over the entire energy range covered by experiment.

The reasons for this failure have been analysed by Walters (1975) and by Hartley and Walters (1988). The rare-gas potentials used in the calculation of singly inelastic cross sections in the first Born approximation are too strong to justify first-order perturbation theory. The truncated basis sets used in the close coupling calculations are not sufficient for a representation of the important reaction channels. Doubly inelastic contributions to the inclusive cross section are, on the other hand, given correctly (Hartley and Walters 1987a) by first-order perturbation theory.

As the relative contribution of the singly inelastic processes to the total inclusive cross sections increases with target size, an improved treatment of these channels is required.

The free-collision model (FCM), first introduced by Dimitriev and Nikolaev (1963), has been demonstrated to yield proper electron loss cross sections for collisions of hydrogen with heavier rare-gas targets (Dewangan and Walters 1978). Results obtained with the impulse approximation (Hartley and Walters 1987b, 1988) lead to excitation and electron loss cross sections for singly inelastic processes, which together with the contributions of doubly inelastic reactions calculated in first Born are in good agreement with the experimental data.

The aim of the present contribution is to demonstrate, that the optical model scheme, previously introduced by Lüdde *et al* (1988) and tested for the case of one-electron collision systems (Ast *et al* 1988), is able to yield singly inelastic excitation and loss cross sections for the systems in question. The one-centre version of the optical model suggested is briefly reviewed in section 2. The results for the collision of H(1s) and of metastable H(2s) with He, Ne and Ar are presented in sections 3 and 4 respectively.

In order to compare our results for electron loss with experiment we add the doubly inelastic contributions obtained by Dewangan and Walters (1978) to our singly inelastic results. Detailed reasons why doubly inelastic processes are not covered by our optical model approach are given in sections 3 and 4. Concerning direct excitation results, we investigate the influence of post-collisional Stark mixing in section 3. Atomic units are used throughout.

2. Review of the optical model

The optical model (first introduced by Feshbach (1958) for the stationary treatment of collision systems) attempts to formulate an exact set of truncated coupled-channel equations including the coupling to the complementary representation space by a complex potential. In practice this aim can only be achieved with some approximations. One possible approximation, the local optical model, in which the perturbative expression for the optical potential is resummed with the assumption that consecutive interactions are essentially instantaneous, was introduced in Lüdde *et al* (1988). The one-centre version leads to a set of coupled-channel equations of the form

$$\dot{\boldsymbol{a}} = \left(\frac{1}{f}(\mathbf{1} - \mathbf{G}^{-1}) - \mathrm{i}\varepsilon\right)\boldsymbol{a}. \tag{4}$$

The vector $\boldsymbol{a}$ denotes the coefficients for the expansion of the time-evolving electron wavefunction of one collision partner (in our case hydrogen) in terms of a finite basis set (P space). ε_{ij} is the corresponding diagonal matrix of the orbital energies and $\mathbf{1}$ is the unit matrix. The complex matrix $\mathbf{G}$ models the coupling of the orbitals included in the representation space to the orbitals not considered explicitly (Q space). The factor f is a scaling factor introduced to improve the energy dependence of the local optical potential.

The matrix representation of the operator $\hat{\mathbf{G}}$ in terms of the P-space orbitals is given by

$$\langle k \mid \hat{\mathbf{G}} \mid j\rangle = \left\langle k \left| \frac{1}{1 + \mathrm{i}f(\hat{V} + \bar{\varepsilon})} \right| j \right\rangle \tag{5}$$

where $\hat{V}$ describes the interaction of the other collision partner with the electron in the hydrogen atom. In the present case we use a frozen screening potential of the rare-gas targets derived from Hartree–Fock densities given by Clementi and Roetti (1974). $\bar{\varepsilon}$ is the weighted average of the energies of the (infinite number) of Q-space orbitals. The results presented below are obtained with the simplest choice $\bar{\varepsilon} = 0$, which is motivated by the results of δ-electron emission in atom–atom collisions (Duncan and Menendez 1979) and supported by the small influence of a consistent evaluation of $\bar{\varepsilon}$ on calculated cross sections as indicated in Ast *et al* (1988).

The fact that we replace the rather involved interaction $\hat{V}$ by an effective (i.e. single-particle) potential implies that we do not incorporate simultaneous doubly inelastic processes. These depend mainly on the electron electron interaction as outlined in the work of Hartley and Walters (1987a,b, 1988).

The set of basis states consists of hydrogen wavefunctions. We have investigated the question of P-space convergence for each collision system carefully and have found a set of 10 states (KLM shell) sufficient for the two sets of initial conditions considered. As higher bound states of the hydrogen atom are not populated after the collision process, we may interpret the Q-space population calculated from the loss of P-space norm as electron loss from the hydrogen projectile or as a measure of the inclusive ionisation probability.

The scaling factor f is fitted at 10 keV amu^{-1} for all collision systems by the procedure outlined in Ast *et al* (1988). With this choice of f the results of the scaled local optical potential calculations are found to coincide with results of the first Born approximation in the high-energy limit for all collision systems investigated. This is

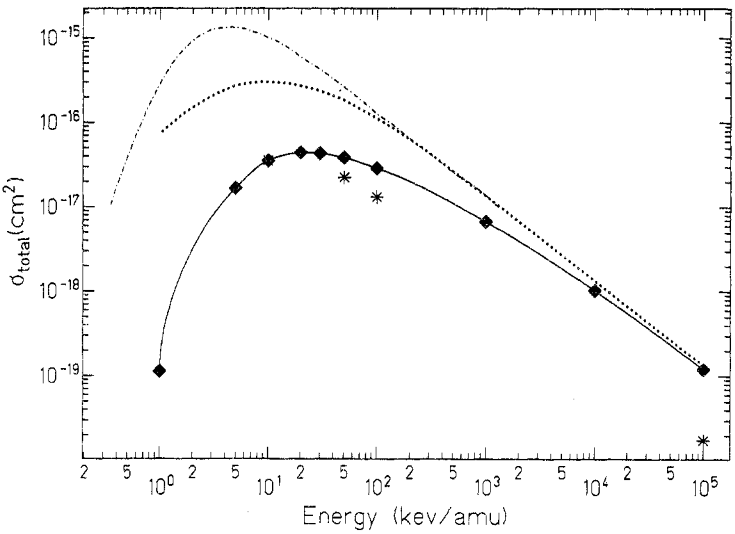

Figure 1. H(1s)+Ar comparison of theoretical approaches for excitation into H(2p): chain curve, first Born approximation unscaled Levy (1969a); dotted curve, AO close coupling with 10 AO centred on hydrogen; full curve, scaled optical model; *, unscaled optical potential ($f = 1$).

illustrated in figure 1 for the example of the 2p excitation cross section of hydrogen colliding with argon atoms in figure 1. In the following we only present results for the scaled optical potential.

The numerical code for the solution of the coupled-channel equations has been described in a previous publication (Ast *et al* 1988). For a screened target potential it is sufficient to start the time integration at an initial separation of $15a_0$. The time evolution of the wavefunction is followed until the the final probabilities $|a_j|^2$ stabilise within a numerical accuracy of five digits. This situation is typically reached at a final internuclear separation of less than $25\,a_0$. No Stark mixing of the final states or spurious long range coupling effects are observed for the screened frozen atomic target potential.

3. Results for hydrogen 1s projectiles

In view of the fact that we calculate cross sections via an effective potential description of the target atoms, our results include only the singly inelastic processes (i), while the inclusive experimental cross sections also include the contributions from doubly inelastic processes (iii). Therefore any serious calculation of singly inelastic cross sections has to predict smaller or at most equal cross sections compared with the inclusive experimental data. In figures 2–4 we present results for the electron loss from hydrogen projectiles colliding with helium, neon and argon targets. We compare the experimental results available with data obtained in first Born approximation (Levy 1969a, Bell *et al* 1969), the free-collision model (Dewangan and Walters 1978) and results obtained with our optical potential model.

The cross sections calculated with the first Born approximation summing over all possible final states of the target (Bell *et al* 1969) or assuming closure (Levy 1969a) are in good agreement in the case of He targets for impact energies larger than

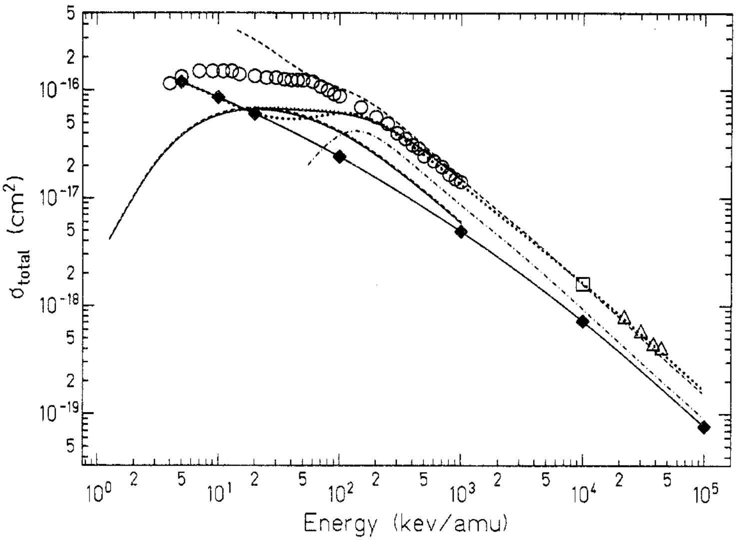

Figure 2. H(1s) + He electron loss. Experiment: ○, Allison (1958); □, Smythe and Toevs (1965); △, Acerbi *et al* (1974). Theory: broken curve, inclusive cross section (FCM); chain curve, doubly inelastic processes (FCM) Dewangan and Walters (1978); broken–full curve, singly inelastic process (first Born approximation); dotted–full curve, inclusive cross section (first Born approximation) Bell *et al* (1969); full curve, optical model (singly inelastic); dotted curve, singly inelastic process (optical model) + doubly inelastic processes (FCM).

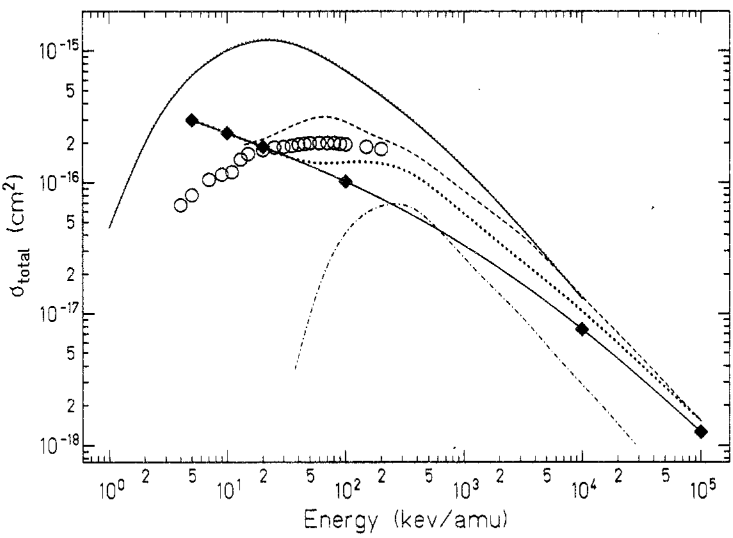

Figure 3. H(1s)+Ne electron loss. Experiment: ○, Allison (1958). Theory: dotted–full curve, first Born approximation with closure Levy (1969a); otherwise, see figure 2.

100 keV amu^{-1}, but overestimate the experimental data for the collisions of hydrogen with neon and argon for all but the highest energies (Levy 1969a). The calculated results of Dewangan and Walters (1978) for inclusive cross sections are in good agreement with the experimental data over the entire energy range.

Our optical model results consistently underestimate the experimental cross sections for impact energies higher than 20 keV amu^{-1}. Our results for energies below 20 keV amu^{-1} have to be treated with caution as the local approximation cannot be maintained if the collision time becomes larger than a typical atomic timescale. The fact that we describe singly inelastic processes in a reasonable fashion is explained by the following statements. In the case of helium targets Bell *et al* (1969) give results for singly inelastic processes alone which are in agreement with our results for energies above 100 keV amu^{-1}. Besides the results for total inclusive cross sections Dewangan and Walters (1978) have calculated results for the summed contribution of doubly inelastic processes. The sum of our optical model results for singly inelastic processes and the doubly inelastic contribution of Dewangan and Walters is in good agreement with the experimental data and the results obtained with the free-collision model.

We note, however, that in figure 4 the electron-loss cross sections for the case of Ar targets do not agree with the results of the free-collision model at high energies. Also the comparison with the first Born approximation of Levy (1969a) is not complete, as these results do not cover the energy region above 20 MeV amu^{-1}. As, however, we obtain the correct Born limit for the excitation channels (see figure 1 for the case of 2p excitation) we expect that we also reproduce the correct Born limit for singly inelastic electron-loss cross sections. The difference with respect to the free-collision model is an open problem.

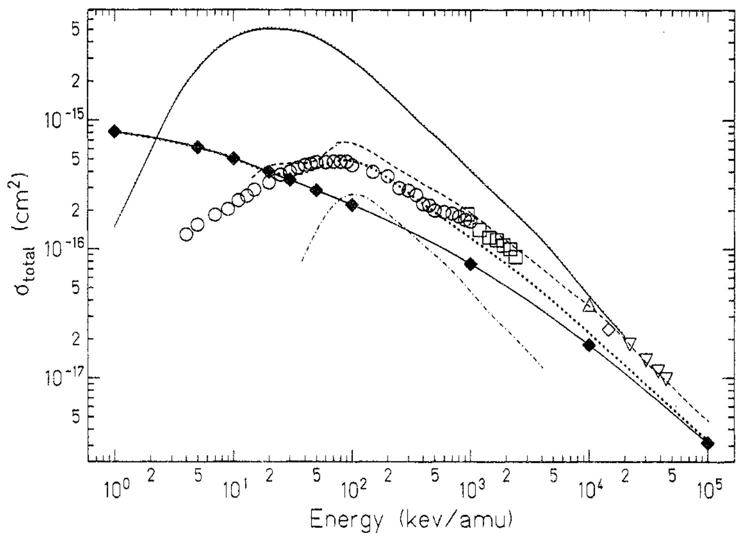

Figure 4. H(1s) + Ar electron loss, Experiment: ○, Allison (1958); □, Toburen *et al* (1968); △, Berkner *et al* (1964); ◁, Smythe and Toevs (1965); ▽, Acerbi *et al* (1974). Theory: see figure 3.

Andersen *et al* (1988) first analysed target and projectile final charge state in a crossed beam experiment for a few energies.

$$\mathrm{H} + \mathrm{A} \rightarrow \mathrm{H}^+ + \mathrm{A}^{q+} + (q+1)\mathrm{e}^- \qquad q = 1, 2. \tag{6}$$

These results are consistent with the picture indicated above and show that this specific doubly inelastic channel gives an important contribution to the difference between singly inelastic processes (i) and the inclusive cross sections.

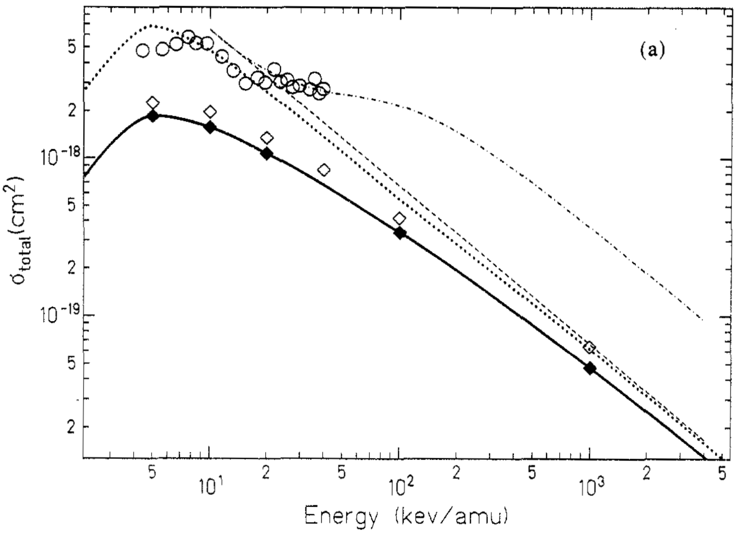

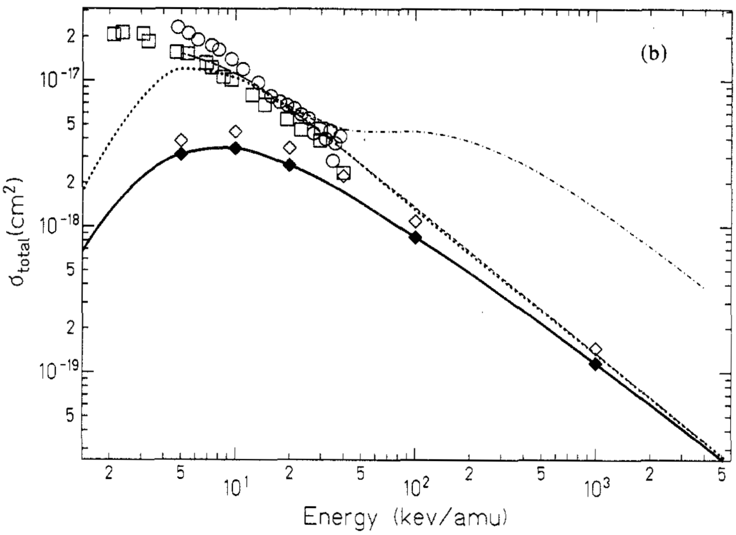

Figure 5. (*a*) H(1s) + He → H(2s) + He. Experiment: ○, Orbeli *et al* (1970). Theory: broken curve, singly inelastic excitation cross section; chain curve, inclusive excitation cross section (first Born approximation) Bell *et al* (1973,1974); dotted curve, AO close coupling; full curve, optical potential model; ◇, optical model with a two-parametric ansatz for the target potential. (*b*) H(1s) + He → H(2p) + He. Experiment: ○, Orbeli *et al* (1970); □, Dose *et al* (1968). Theory: see (*a*).

In comparing our results obtained for the three different rare gas targets we note that the relative contribution of singly inelastic processes to the inclusive electron-loss cross sections increases with increasing target charge. This is in accord with statements given by other authors (Dewangan and Walters 1978, Hartley and Walters 1988). We further note that none of the theoretical approaches is able to reproduce the electron-loss data for hydrogen–helium collisions below 50 keV amu^{-1} impact energy.

In figures 5–7 we show the total cross sections for the excitation into the 2s (figures (*a*)) and 2p (figures (*b*)) states of hydrogen in collision with helium, neon and argon. In each case we show results obtained in the first Born approximation (Levy 1969

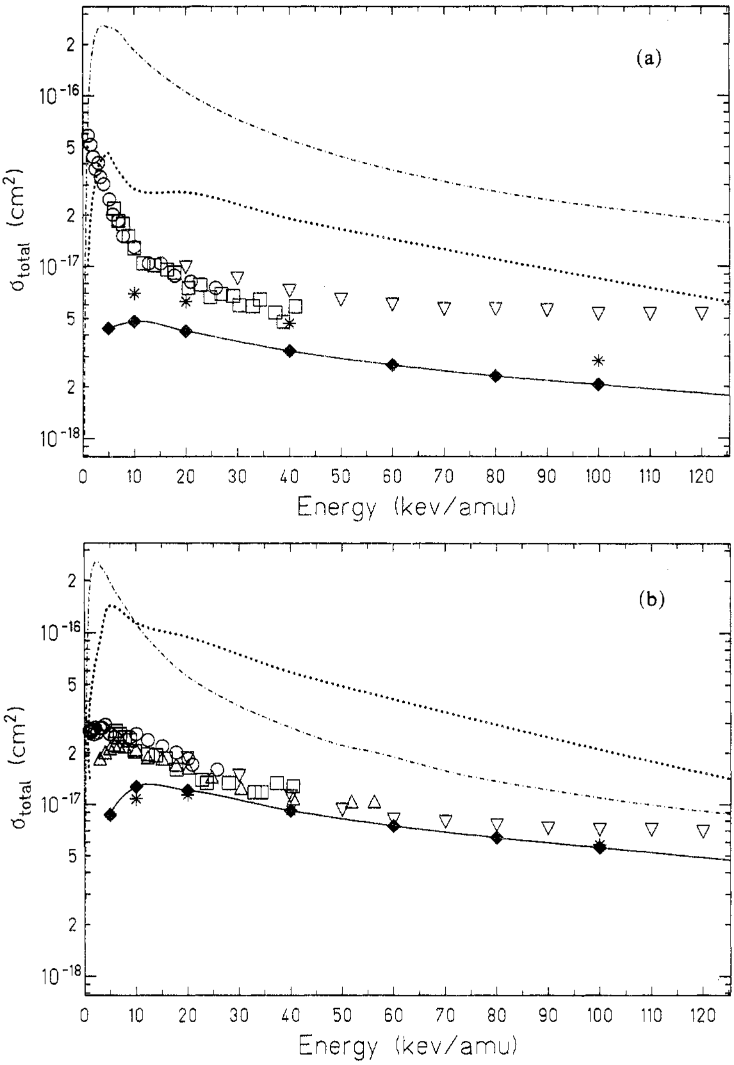

Figure 6. (*a*) H(1s) + Ne → H(2s) + Ne. Experiment: ○, Birely and McNeal (1972); □, Orbeli *et al* (1970); △, Hughes and Choe (1972b). Theory: chain curve, first Born unscaled Levy (1969a); dotted curve, AO close coupling; full curve, optical model; *, optical model with Stark mixing. (*b*) H(1s) + Ne → H(2p) + Ne. Experiment: ○, Birely and McNeal (1972); □, Orbeli *et al* (1970); △, Dose *et al* (1968); ▽, Hughes and Choe (1972a). Theory: see (*a*).

a,b, Bell *et al* 1973,1974), results obtained in a standard close coupling calculation (our calculation, using a ten-states (KLM shell) basis set centred on hydrogen), which agrees closely with the results by Flannery (1969) and Levy (1969b) for the He target and reasonably with the results using a smaller basis set for Ne and Ar by Levy (1970) and our optical model results in comparison with the experimental data available. Looking first at the Born and close coupling results for the singly inelastic processes, we note a good agreement for energies smaller than 20 keV amu^{-1} and underestimation at higher energies. Summing over all possible final states of the helium target leads to good agreement over the entire energy range for results obtained with the first

Born approximation (Hartley and Walters 1987a). Results obtained with a molecular approach by Kimura and Lane (1987) are in good agreement with the experimental data. By contrast one finds consistent overestimation of the experimental results for Ne and Ar targets by first Born and AO close coupling calculations. Slightly improved Born approximation results are obtained by the introduction of a velocity-dependent scaling parameter (fitted with the experimental detected hydrogen electron-loss cross sections) for the case of Ne, but this procedure fails for the argon target (Levy 1969a). Discarding again optical model results below 20 keV amu^{-1} we see that our excitation cross sections for collisions with helium targets underestimate the experimental data again (due to the neglect of doubly inelastic processes for higher energies). Our optical model results agree with the Born and close coupling data for singly inelastic processes for energies above 200 keV amu^{-1}. For collisions with neon and argon the 2p excitation cross sections of the hydrogen projectile obtained with the optical potential model are in good agreement with the experimental data, while our optical model results underestimate the 2s excitation cross sections. We can understand this discrepancy by the following argument. If the target atom is ionised simultaneously with the excitation of the hydrogen near the closest approach of the two atoms, a long-range Coulomb potential of the target ion will influence the projectile in the outgoing channel, and Stark mixing occurs, especially between the 2s and 2p states.

In order to demonstrate that this argument is reasonable, we made the following rough calculation. As our calculated singly inelastic electron-loss cross sections underestimate the inclusive experimental data due to the lack of doubly inelastic processes, we assume that the difference between the experimental and our theoretical cross sections is the contribution of the doubly inelastic process

$$\mathrm{H(1s)} + \mathrm{A} \rightarrow \mathrm{H}(nl) + \mathrm{A}^{+} + \mathrm{e}^{-} . \qquad (7)$$

We further assume that the ionisation probability for the rare gas has the same functional dependence on the impact parameter as the ionisation of the hydrogen. When we switch over from the neutral atomic target potential to a singly charged rare-gas potential at the closest approach, we obtain cross sections (asterisks) which indicate that Stark mixing of hydrogen projectile states by an ionic rare-gas potential is able to explain the discrepancies. The 2s cross sections are increased whereas the 2p excitation cross sections of hydrogen do not change considerably.

Our 2s excitation cross section in hydrogen–neon collisions decreases with increasing energy still a little faster than the experimental results. This might be explained by the contribution of the part of doubly inelastic processes in which both colliding partners are excited

$$\mathrm{H} + \mathrm{A} \rightarrow \mathrm{H}^{*} + \mathrm{A}^{*} . \qquad (8)$$

As we have seen this doubly inelastic channel is the dominant one in hydrogen–helium collisions and responsible for the differing slopes of the experimental data and the curve of our calculated singly inelastic cross sections. So it is not unreasonable to assume that this type of process will occur in hydrogen–neon collisions too.

We confirm the finding of Hartley and Walters (1987b) that with increasing target size the singly inelastic processes grow relative to the doubly inelastic cross sections. In particular, the excitation cross sections for hydrogen atoms colliding with argon are dominated by the singly inelastic process, while in hydrogen–helium collisions

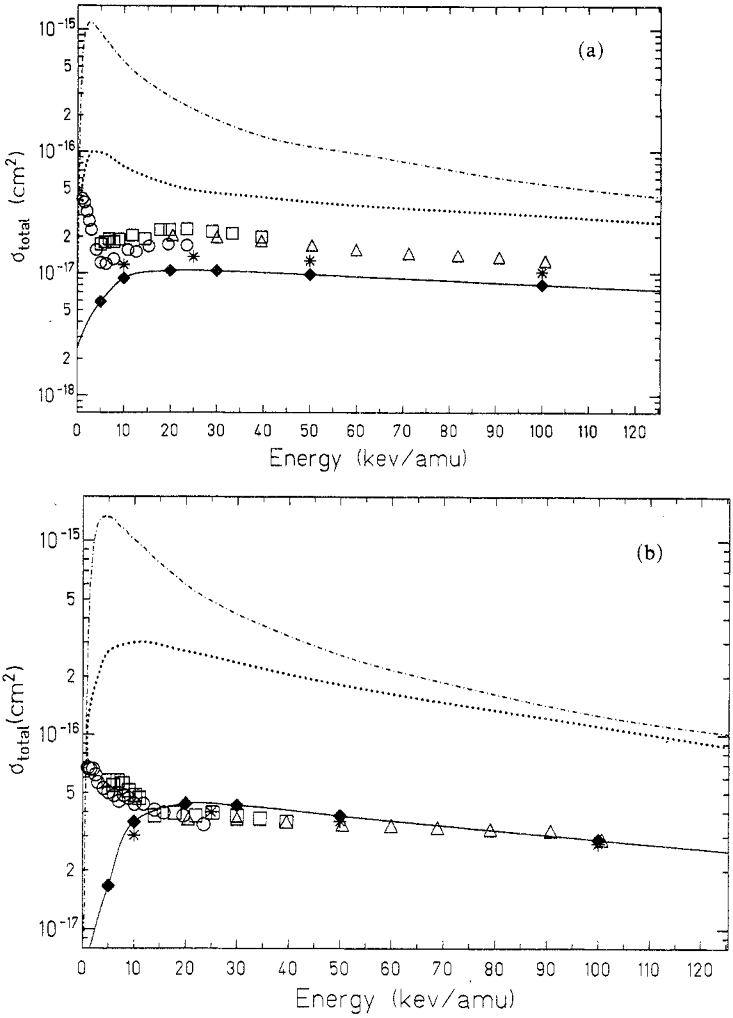

Figure 7. (*a*) H(1s) + Ar → H(2s) + Ar. (*b*) H(1s) + Ar → H(2p) + Ar, see figure 6.

hydrogen excitation cross sections are dominated by the doubly inelastic processes. The question whether singly or doubly inelastic processes are more important in a collision system cannot be answered by the comparison of the binding energies of the outer shell electrons of the colliding partners. This argument would lead to the assumption that in hydrogen–argon collisions doubly inelastic processes should be more important than in hydrogen-helium collisions as the 3p argon electron posesses a binding energy of −0.59 au compared to the helium 1s electron's energy of −0.91 au (Hartree–Fock binding energies, Clementi and Roetti 1974).

Taking into account the results for all the three-collision systems investigated here, several facts indicate that the collision of hydrogen atoms with helium plays a particular role. In contrast to the hydrogen–neon and hydrogen–argon collisions no theoretical calculation agrees with the experimental data for electron loss at energies lower than 50 keV amu^{-1}. The results obtained in an AO close coupling calculation and the optical potential model are strongly dependent on the effective potential used for the description of the the helium target. An effective potential calculated from the simple variational ansatz

$$\Psi(r_1, r_2) = a[\exp(\alpha_1 r_1 + \alpha_2 r_2 + \exp(\alpha_2 r_1 + \alpha_1 r_2)] \tag{9}$$

which decreases more slowly than the Hartree–Fock potential increases the cross sections by about 25–30%.

4. Collision of metastable hydrogen atoms with rare gases

The collisional destruction of the metastable hydrogen 2s state has been the subject of several investigations. The most important reaction channel is the loss of the electron

$$\mathrm{H(2s)} + \mathrm{A} \rightarrow \mathrm{H}^+ + \mathrm{A}^* + \mathrm{e}^- \ . \tag{10}$$

For lower energies de-excitation directly to the ground state or via several excited states plays an important role as well (Gilbody *et al* 1970, Gilbody and Corr 1974, McKee *et al* 1979, Hill *et al* 1979):

$$\begin{aligned} \mathrm{H(2s)} + \mathrm{A} &\rightarrow \mathrm{H(1s)} + \mathrm{A}^* \\ &\rightarrow \mathrm{H}(nl) + \mathrm{A}^* \rightarrow \mathrm{H(1s)} + \mathrm{A}^* \ . \end{aligned} \tag{11}$$

Even the collisional attachment of an electron and sucsessive decay of the unstable excited H^- ion play a role (Hill *et al* 1980)

$$\begin{aligned} \mathrm{H(2s)} + \mathrm{A} \rightarrow \mathrm{H}^{-^*} + \mathrm{A}^* &\rightarrow \mathrm{H(1s)} + \mathrm{A}^+ + \mathrm{e}^- \\ &\rightarrow \mathrm{H(1s)} + \mathrm{A}^* \ . \end{aligned} \tag{12}$$

The formation of stable H^- ions occurs rather rarely (Hill *et al* 1979 a,b)

$$\mathrm{H(2s)} + \mathrm{A}^+ \rightarrow \mathrm{H}^- + \mathrm{A}^+ \ . \tag{13}$$

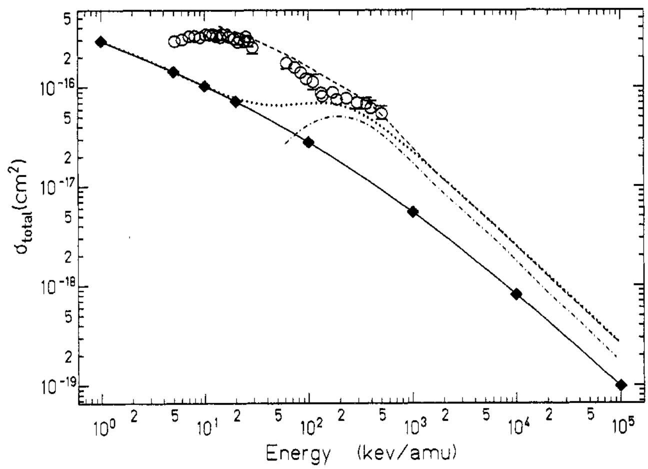

Figure 8. H(2s) + He electron loss. Experiment: ○, Gilbody and Corr (1974). Theory: broken curve, inclusive cross section (FCM); chain curve, doubly inelastic cross section (FCM) Dewangan and Walters (1978); full curve, optical model (singly inelastic); dotted curve, singly inelastic process (optical model) + doubly inelastic processes (FCM).

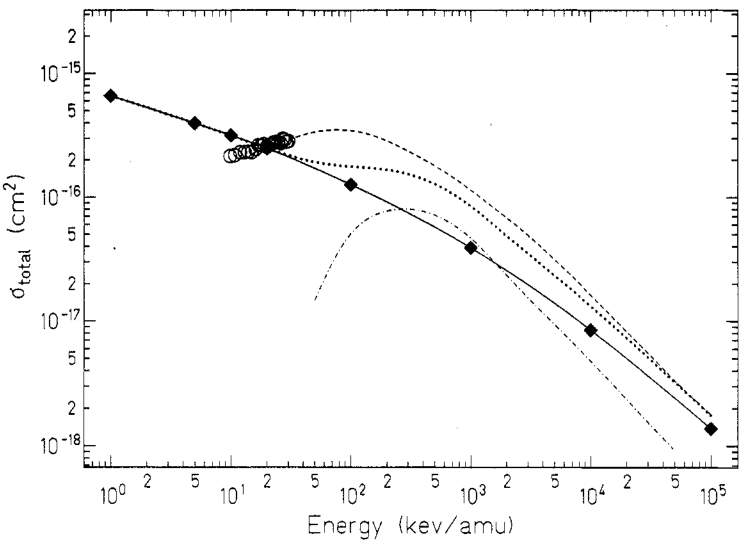

Figure 9. H(2s) + Ne electron loss. Experiment: ○, Gilbody *et al* (1971). Theory: see figure 8.

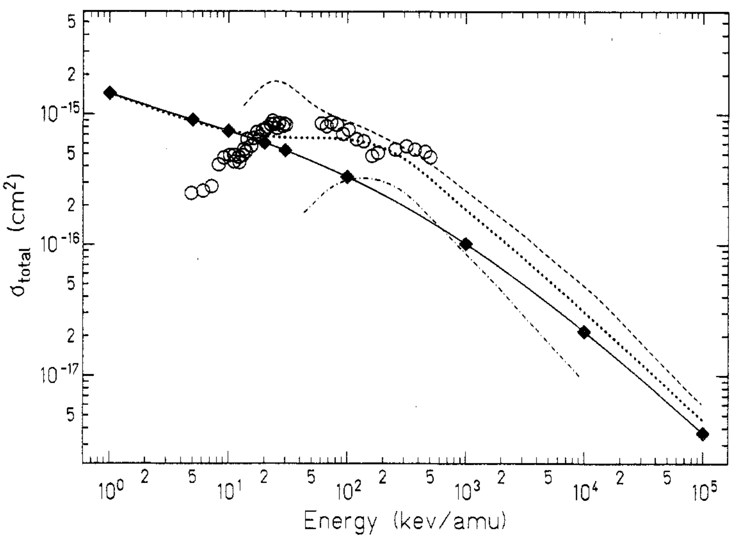

Figure 10. H(2s) + Ar elctron loss, see figure 8.

In all of these reactions the rare-gas target may remain in its ground state (singly inelastic process) or could be excited or ionised (doubly inelastic process). We present results for the singly inelastic contribution to the first two reactions.

The electron loss from the metastable hydrogen in collision with helium, neon and argon is shown in figures 8–10. The results are definitly related to the results for the electron loss from the ground state shown in section 3. Our optical model results for the singly inelastic process underestimate the global experimental data for energies larger than 20 keV amu^{-1} for neon and argon targets and 2 keV amu^{-1} for

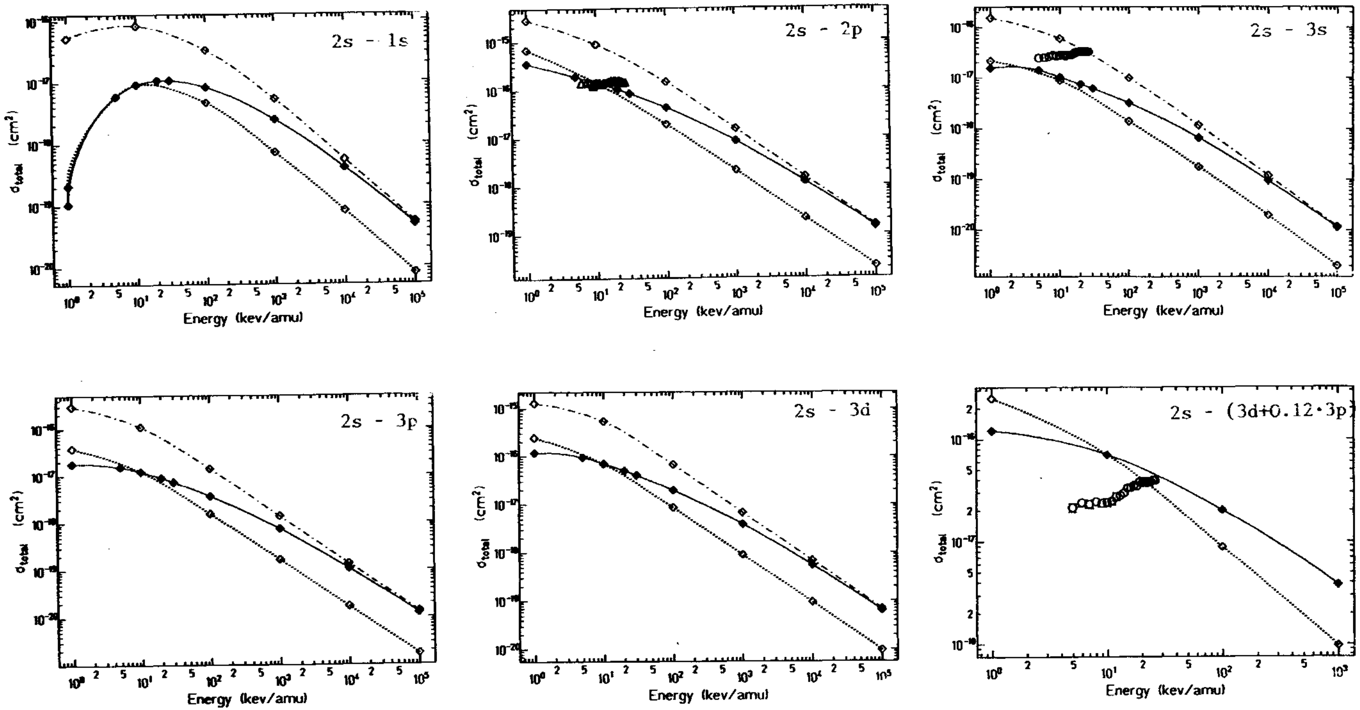

Figure 11. H(2s) + Ar → H(nl) + Ar. Experiment: △, McKee *et al* (1979); ○, Hill *et al* (1980). Theory: chain curve, AO close coupling; dotted curve, unscaled optical potential model; full curve, optical model.

helium respectively. If we add Dewangan and Walter's (1978) results obtained with the free-collision model for the doubly inelastic reaction to our exclusive singly inelastic results, we find good agreement with Dewangan and Walters global results and the experimental data. One finds again that for high energies doubly inelastic processes become less important with increasing charge of the target nucleus.

Figure 11 shows the cross section for the transition from the 2s to other bound states in collision of hydrogen with argon. A comparison with experimental data (McKee *et al* 1979, Hill *et al* 1980) is only possible for a small range of energies. There the agreement between the experimental data and our results is rather poor, as doubly inelastic processes contribute particularly in this energy region. It would be very instructive to have data for a wider energy range and explicit measurements of the singly inelastic channels in order to seperate more clearly the contribution of singly and doubly inelastic processes to the global cross sections.

Tables 1 and 2 contain the transition cross sections for collisions with helium and neon.

Table 1. Total excitation cross sections (cm^2) for metastable 2s hydrogen atoms colliding with helium.

Energy (keV amu^{-1})	σ_{1s}	σ_{2p}	σ_{3s}	σ_{3p}	σ_{3d}
	AO close coupling				
100000.00	0.638E-21	0.133E-20	0.110E-21	0.125E-21	0.604E-21
1000.00	0.607E-19	0.133E-18	0.106E-19	0.126E-19	0.606E-19
100.00	0.603E-18	0.133E-17	0.105E-18	0.126E-18	0.607E-18
10.00	0.512E-17	0.132E-16	0.987E-18	0.125E-17	0.611E-17
1.00	0.367E-18	0.136E-15	0.569E-17	0.103E-16	0.470E-16
	Unscaled optical potential ($f = 1$)				
4000.00	0.320E-20	0.135E-19	0.162E-19	0.157E-20	0.618E-20
500.00	0.254E-19	0.107E-18	0.990E-19	0.119E-19	0.492E-19
100.00	0.125E-18	0.532E-18	0.307E-18	0.556E-19	0.243E-18
50.00	0.246E-18	0.106E-17	0.444E-18	0.108E-18	0.484E-18
10.00	0.107E-17	0.514E-17	0.790E-18	0.504E-18	0.239E-17
	Optical potential				
100000.00	0.638E-21	0.133E-20	0.110E-21	0.125E-21	0.604E-21
10000.00	0.581E-20	0.128E-19	0.103E-20	0.121E-20	0.585E-20
1000.00	0.508E-19	0.115E-18	0.914E-20	0.108E-19	0.527E-19
100.00	0.359E-18	0.873E-18	0.691E-19	0.815E-19	0.401E-18
30.00	0.884E-18	0.229E-17	0.589E-18	0.213E-18	0.104E-17
20.00	0.112E-17	0.310E-17	0.242E-18	0.287E-18	0.144E-17
10.00	0.163E-17	0.514E-17	0.395E-18	0.469E-18	0.239E-17
5.00	0.191E-17	0.830E-17	0.626E-18	0.729E-18	0.387E-17
1.00	0.175E-18	0.231E-16	0.115E-17	0.162E-17	0.833E-17

5. Conclusion

The electron loss from the hydrogen projectiles in collision with rare gases is an important reaction channel. The neglect of this channel in the standard AO close coupling calculations leads to incorrect results for excitation cross sections in collision with neon

Table 2. Total excitation cross sections (cm^2) for metastable 2s hydrogen atoms colliding with neon.

Energy (keV amu^{-1})	σ_{1s}	σ_{2p}	σ_{3s}	σ_{3p}	σ_{3d}
100000.00	0.932E-20	0.197E-19	0.157E-20	0.189E-20	0.901E-20
10000.00	0.775E-19	0.169E-18	0.135E-19	0.161E-19	0.774E-19
1000.00	0.494E-18	0.118E-17	0.936E-19	0.111E-18	0.543E-18
100.00	0.215E-17	0.624E-17	0.478E-18	0.549E-18	0.288E-17
30.00	0.384E-17	0.133E-16	0.107E-17	0.123E-17	0.618E-17
20.00	0.441E-17	0.169E-16	0.126E-17	0.156E-17	0.789E-17
5.00	0.446E-17	0.360E-16	0.236E-17	0.311E-17	0.171E-16
1.00	0.165E-18	0.787E-16	0.307E-17	0.493E-17	0.282E-16

and argon targets. The global inclusion of electron loss via an optical model leads to improved results for excitation and ionisation cross sections. As we have calculated only contributions of singly inelastic processes where the rare-gas target remains in its ground state, our results for electron loss usually underestimate the experimental data which correspond to the sum of singly inelastic and all doubly inelastic processes. When we add the doubly inelastic contributions obtained with the free-collision model of Dewangan and Walters (1978) to our results, we are in good agreement with the experimental data.

There is also good agreement between the experimental data and our results for the excitation into the 2p state whereas we underestimate the excitation cross section for the 2s state. We have indicated that a simultaneous ionisation of the target rare gas in the collision leads to a Stark mixing between the 2s and 2p state in the outgoing channel which removes this discrepancy. For helium targets the doubly inelastic processes are more important while the singly inelastic processes become dominant for increasing target charge.

In the case of metastable hydrogen 2s projectiles the doubly inelastic processes are more important in comparison with the collision of ground-state hydrogen with rare gases.

Acknowledgments

We would like to thank the Deutsche Forschungsgemeinschaft (DFG) for partial financial support and the Gesellschaft für Schwerionenforschung (GSI) for making its computer facilities available.

References

Acerbi E, Birattari C, Candoni B, Castiglioni M, Cutrupi D and Succi C 1974 *Lett. Nuovo Cim.* **10** 598–602

Allison S K 1958 *Rev. Mod. Phys.* **30** 1137–68

Andersen L H, Nielsen L B and Sorensen J 1988 *J. Phys. B: At. Mol. Opt. Phys.* **21** 1587–1602

Ast H, Lüdde H J and Dreizler R M 1988 *J. Phys. B: At. Mol. Opt. Phys.* **21** 4143–56

Barnett C F and Reynolds H K 1958 *Phys. Rev.* **109** 355–9

Bell K L, Dose V and Kingston A E 1969 *J. Phys. B: At. Mol. Phys.* **2** 831–8

Bell K L and Kingston A E 1971 *J. Phys. B: At. Mol. Phys.* **4** 162–7

Bell K L, Kingston A E and McIlveen W A 1973a *J. Phys. B: At. Mol. Phys.* **6** 1237–45

—— 1973b *J. Phys. B: At. Mol. Phys.* **6** 1246–1254
Bell K L, Kingston A E and Winter T G 1974 *J. Phys. B: At. Mol. Phys.* **7** 1369–84
Berkner K H, Kaplan S N and Pyle R V 1964 *Phys. Rev.* **134** 1461–4
Birely J H and McNeal R J 1972 *Phys. Rev.* A **5** 257–65
Clementi E and Roetti C 1974 *At. Data Nucl. Data Tables* **14** 177–478
Dewangan D P and Walters H R J 1978 *J. Phys. B: At. Mol. Phys.* **11** 3983–4017
Dimitriev I S and Nikolaev V S 1963 *Sov. Phys.-JETP* **17** 447–50
Dose V, Gunz R and Meyer V 1968 *Helv. Phys. Acta* **14** 269–73
Duncan M M and Menendez M G 1979 *Phys. Rev.* A **19** 49–54
Flannery M R 1969 *J. Phys. B: At. Mol. Phys.* **2** 913–922
Gilbody H B, Browning R, Reynolds R M and Riddell G I 1971 *J. Phys. B: At. Mol. Phys.* **4** 94–105
Gilbody H B and Corr J L 1974 *J. Phys. B: At. Mol. Phys.* **7** 1953–67
Hartley H M and Walters H R J 1987a *J. Phys. B: At. Mol. Phys.* **20** 1983–2003
—— 1987b *J. Phys. B: At. Mol. Phys.* **20** 3811–31
—— 1988 *J. Phys. B: At. Mol. Opt. Phys.* **21** L43-7
Hill J, Geddes J and Gilbody H B 1979a *J. Phys. B: At. Mol. Phys.* **12** L653–5
—— 1979b *J. Phys. B: At. Mol. Phys.* **12** 3341–8
—— 1980 *J. Phys. B: At. Mol. Phys.* **13** 951–8
Hughes R H and Choe S S 1972a *Phys. Rev.* A **5** 656–9
—— 1972b *Phys. Rev.* A **5** 1758–63
Hughes R H, Petefish H M and Kisner H 1972 *Phys. Rev.* A **5** 2103–6
Kimura M and Lane N F 1988 *Phys. Rev.* A **37** 2900–5
Levy H II 1969a *Phys. Rev.* **185** 7–15
—— 1969b *Phys. Rev.* **187** 136–42
—— 1970 *Phys. Rev.* A **1** 750–4
Lüdde H J, Ast H and Dreizler R M 1988 *J. Phys. B: At. Mol. Opt. Phys.* **21** 4131–41
McKee J D A, Geddes J and Gilbody H B 1979 *J. Phys. B: At. Mol. Phys.* **12** 1701–9
Orbeli A L, Andreev E P, Ankudinov V A and Dukelskii V M 1970 *Sov. Phys.-JETP* **30** 63–7
Smythe R and Toevs J W 1965 *Phys. Rev.* **139** 15–18
Stier P M and Barnett C F 1956 *Phys. Rev.* **103** 896–907
Toburen L H, Nakai M Y and Langly R A 1968 *Phys. Rev.* **171** 114–22
Walters H R J 1975 *J. Phys. B: At. Mol. Phys.* **8** L54–7